Bulletin of the *Transilvania* University of Braşov • Vol. 18(67) No. 1 – 2025
Series I: Engineering Sciences
https://doi.org/10.31926/but.ens.2025.18.67.1.2

ENHANCING DERMOSCOPY SEGMENTATION ACCURACY: AN ALGORITHMIC APPROACH FOR AUTOMATIC HAIR REMOVAL FOR SKIN CANCER DETECTION

Dana Elena ILEA GHIȚĂ[1]

Abstract: *This paper presents an automated approach for hair removal in dermoscopy images to enhance the accuracy of skin cancer detection and segmentation. Traditional dermoscopic segmentation often faces challenges due to the presence of hair, which can generate false positives and obscure critical features of the lesion. This paper proposes an algorithm that effectively identifies and removes hair from skin cancer images, enabling clearer visualization of the skin's surface. This method combines image processing techniques with image reconstruction models to distinguish between hair and skin tissue, ensuring minimal distortion of the underlying skin features. The numerical results demonstrate significant improvements in the performance of automated skin cancer detection systems, highlighting the potential of this approach for clinical applications in dermatology.*

Key words: *dermoscopy, skin cancer segmentation, automated hair removal, HAM10000 database*

1. Introduction

Skin cancer is the 17th most common type of cancer, affecting both men and women equally. In 2022, there were 331,722 new cases of skin cancer worldwide, with 179,953 new cases diagnosed in men and 151,769 new cases in women. The World Cancer Research Fund indicated that 58,667 deaths were due to skin cancer in 2022 [17]. It's important to note that these statistics pertain to melanoma, the most serious form of skin cancer. Non-melanoma skin cancers, such as basal cell carcinoma and squamous cell carcinoma, are more common but less likely to be fatal. Thus, early detection is crucial. Image processing techniques play an essential role in the detection of lesions in dermoscopy images. Automated algorithms can analyse dermoscopy images quickly and consistently, reducing human error and enabling faster diagnosis. This is especially valuable in areas with limited access to dermatologists or in situations where a second opinion is needed. Dermoscopy images often contain various challenges such as thick

[1] Faculty of Electrical Engineering and Computer Science, *Transilvania* University of Braşov.

hair, fuzzy borders, complex skin textures, including variations in pigmentation and patterns, noise from imaging devices, irregular illumination conditions and other artefacts that can obscure critical features of the lesion. Image pre-processing techniques help enhance the contrast and clarity of the image, making it easier to distinguish between healthy skin and abnormal areas. These challenges highlight the need for advanced and robust segmentation algorithms that can adapt to different scenarios and account for variations in lesion appearance, image quality, and environmental factors.

One of the primary challenges in dermoscopic analysis is represented by the interference of hair, which can obscure key features of the lesion, making it difficult for clinicians and automated segmentation systems to accurately assess the skin's surface. Hair in dermoscopy images can significantly complicate lesion detection, potentially leading to misdiagnosis or delayed treatment. To address this issue, this paper proposes a pre-processing algorithm for the automatic removal of hair from dermoscopy images. By leveraging advanced image processing techniques, this algorithm efficiently isolates and eliminates hair artefacts while preserving the integrity of the underlying skin features. This pre-processing step not only enhances the clarity of lesions but also improves the accuracy of subsequent image analysis, such as lesion segmentation and classification, which are crucial steps for skin cancer detection.

1.1. Current trends in hair removal in skin cancer images

The automatic removal of hair from dermoscopy images is an active area of research, driven by the need to improve the accuracy of skin cancer detection and analysis. Several image processing techniques have emerged to address this challenge, combining modern deep-learning based methods with traditional image processing operations. With reference to the deep-learning based methods, convolutional neural networks are trained to distinguish between skin lesions and hair, isolating the hair artefacts for removal while preserving lesion details. Recent representative algorithms that belong to this category can be found in references from [1-3], [5], [7], [10-11], [13-14]. The main disadvantage of these methods is that they are sensitive to the training data. The second category of algorithms are based on more traditional image processing methods including morphological image processing methods, edge detection and filtering, adaptive thresholding, segmentation-based techniques and texture analysis [4], [6], [8] and [12]. Lee et al. [8] proposed a benchmark method for hair removal called DullRazor®, whose key features include a morphological closing operation to identify dark hair locations, the use of bilinear interpolation for the replacement of pixels that belong to hair features and a smoothing procedure applied to the resulting image using a median filter. While the DullRazor® algorithm offers several advantages for hair removal in dermoscopy images, it also has some limitations and potential disadvantages: dependency on the accuracy of the hair detection step, loss of fine details (as the interpolation technique used to replace the hair regions with surrounding skin texture may sometimes result in the loss of fine details in the lesion, particularly at the edges), potential over-smoothing and limited generalisation across datasets with

different complexity.

The algorithm proposed in this paper is analysed in the context of skin cancer image segmentation, namely lesion detection. It belongs to the second category of hair removal algorithms and has a dual purpose. First, we focus on presenting the automatic hair removal procedure and use it in conjunction with a well-known segmentation method for quantifying the loss in performance generated by the existent hair in skin cancer images. Second, a numerical quantification for optimising the parameters of the hair removal algorithm is applied to attain complete automation. The numerical quantification is performed on representative images from HAM10000 dataset that comes with a set of Ground Truth data created by a single dermatologist [16]. These binary segmentation masks from the HAM10000 dataset are used in this evaluation.

2. Skin Cancer Images Hair Removal Procedure

Hair removal in dermoscopy images is crucial for accurate melanoma segmentation, as it can significantly interfere with the analysis and identification of lesions. As it can be observed in Figure 1, hair often obscures key features of skin lesions, especially when it overlaps or lies on the melanoma lesion. This makes it difficult for both automated systems and clinicians to accurately identify the boundaries of the lesion.

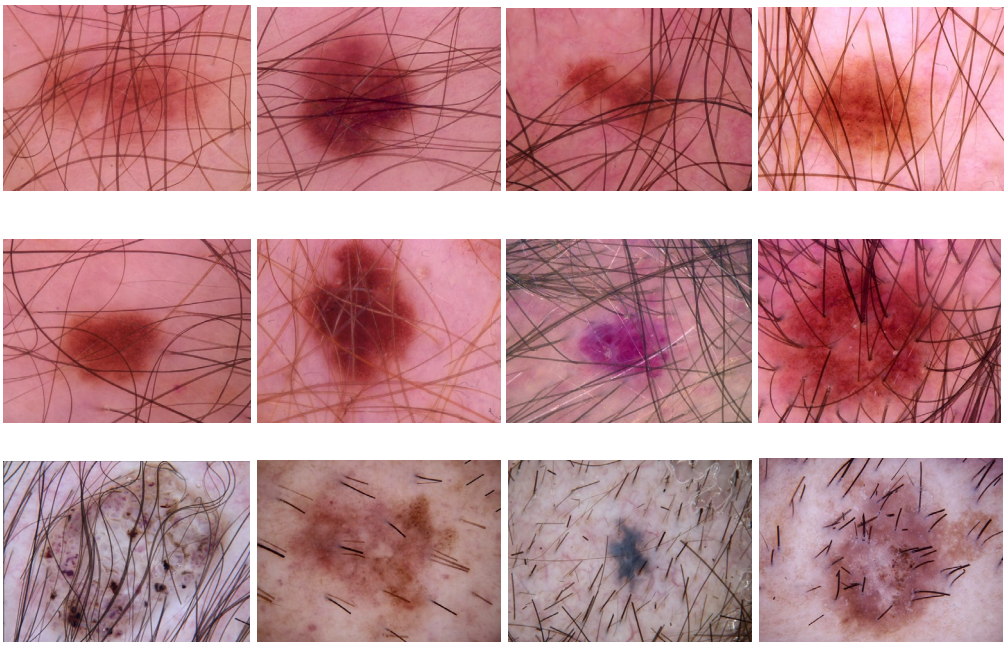

Fig. 1. *Selection of skin cancer images that illustrates the presence of hair. These images are extracted from the HAM10000 Database [16], a large collection of dermoscopic images of pigmented skin lesions*

The presence of hair can create false positives (incorrectly identifying hair as part of the lesion) or false negatives (missing portions of the lesion because they are hidden

under hair). These errors can significantly reduce the accuracy of melanoma detection segmentation procedure. By eliminating hair, the likelihood of these errors is reduced, resulting in more reliable segmentation and diagnosis. The hair extraction in this paper is performed by combining morphological operations followed by image restoration by inpainting. The block diagram of this algorithm is displayed in Figure 2.

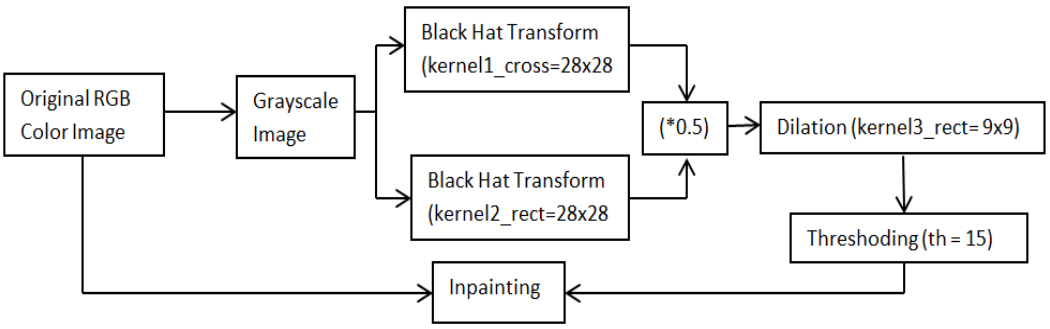

Fig. 2. *Diagram of the skin cancer hair removal procedure*

2.1. The application of morphological operations to extract the hair features

2.1.1. The original image is first converted to the single channel grayscale image representation.

2.1.2. The next step of the hair removal algorithm involves morphological operations to enhance and extract specific features. Two Black Hat transformations are being applied to the grayscale image with the purpose of highlighting the dark regions in an image, particularly those that are surrounded by brighter regions. It works by subtracting the result of the dilation of the image from the original image. Essentially, the Black Hat transform is useful for detecting dark features (such as thin dark hair) that contrast against a brighter background. The first Black Hat transform uses a 28x28 rectangular structuring element (kernel), while the second Black Hat transform uses a cross-shaped structuring element (kernel2). The choice of two different kernels allows the algorithm to detect dark features in different shapes. The two results of the Black Hat transform are averaged to ensure that both contribute equally to the final output, which improves the overall feature detection. This step allows capturing a wider range of dark thin features in the image.

2.1.3. The next step is the application of the dilation operation. Dilation works by expanding the brighter areas of the image, thereby thickening the white regions and making them more pronounced. This step involves a rectangular structuring element set to size 9x9 (kernel3). This was experimentally set, the procedure and numerical results being detailed in Section 3 of this paper.

2.2. Image reconstruction by inpainting

The image resulting from the previous step is converted to a binary image based on a threshold value (experimentally set to the value 15, the selection criteria detailed in Section 3 of this paper). The result of this operation is a binary mask where areas that were determined to be hair features in the black hat image will be set to foreground (255) and the rest will be set to background (0). The next step consists of a procedure called inpainting [15] that fills the foreground in the mask image with image data from adjacent regions from the original image. The white areas (255) in this binary mask indicate the regions to be inpainted. The Navier-Stokes inpainting algorithm was employed as it is particularly useful for filling missing areas with smooth and coherent texture.

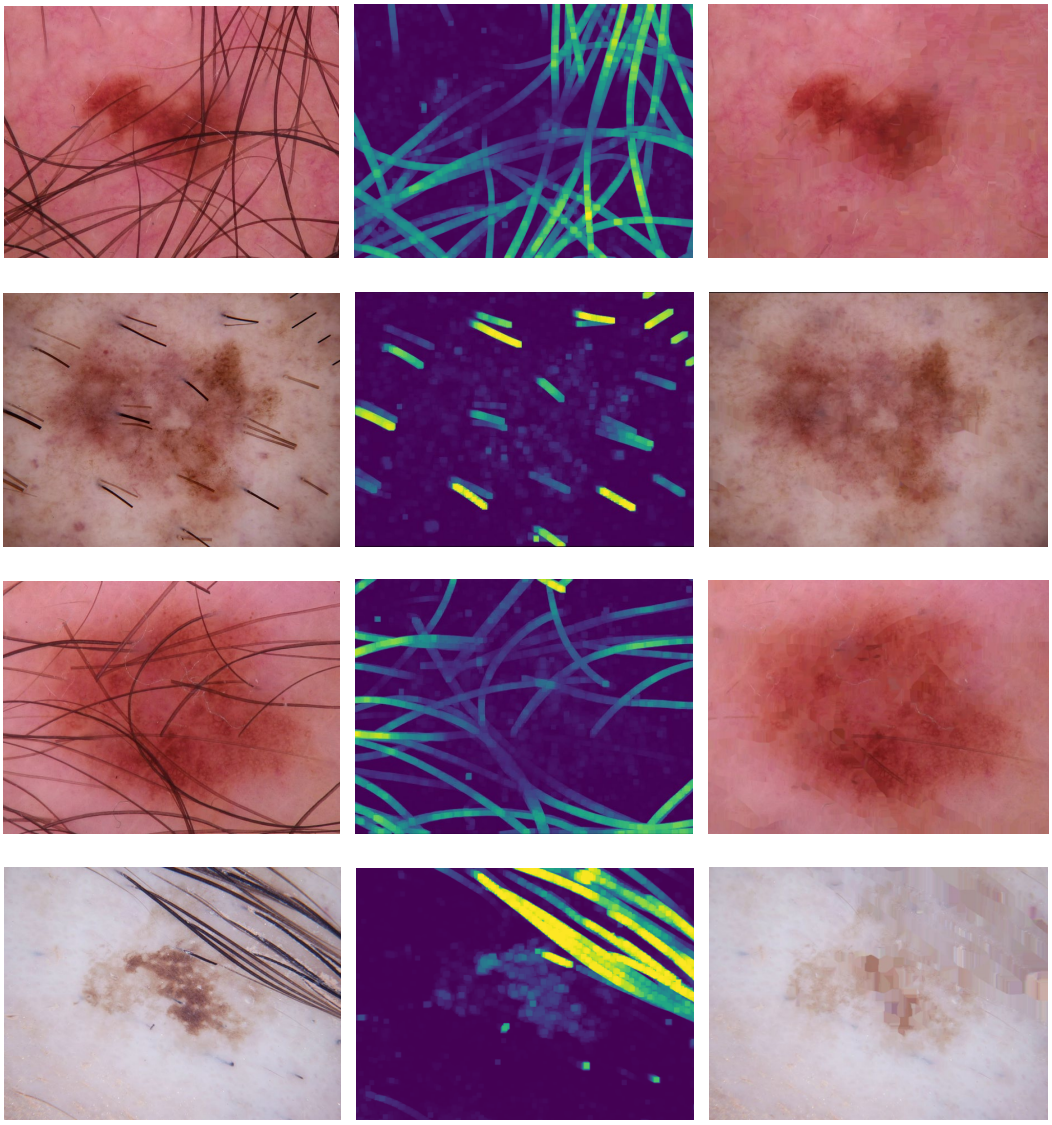

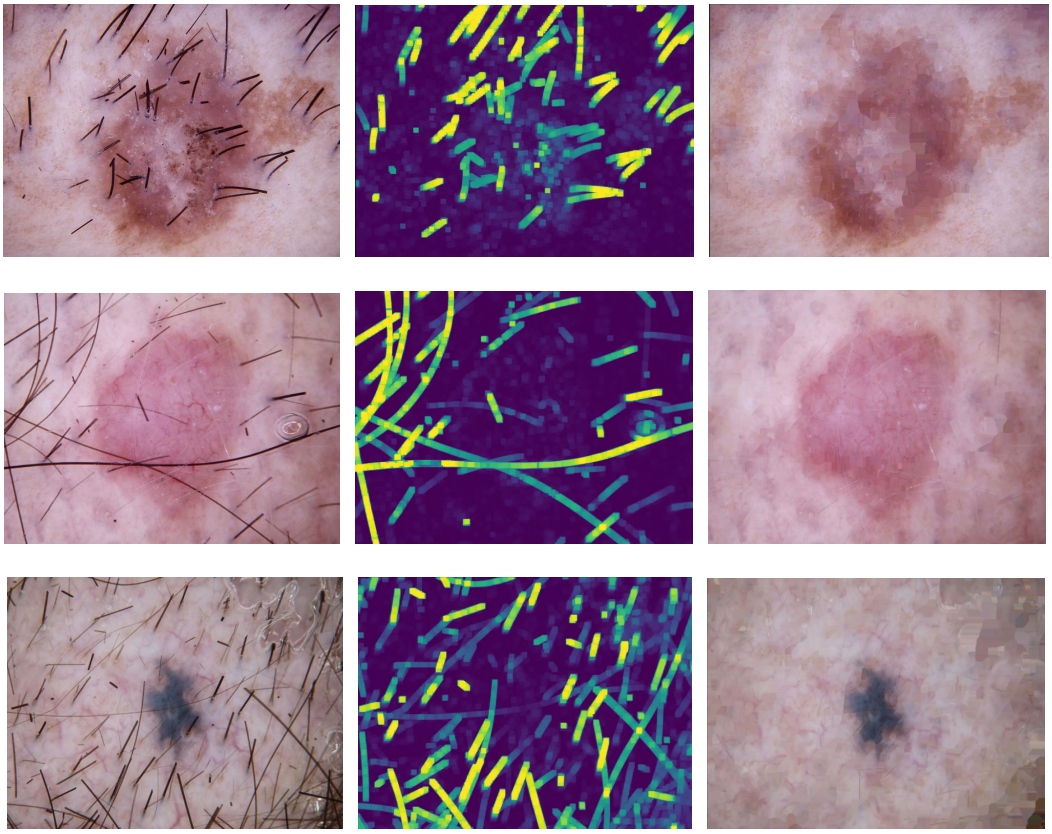

Fig. 3. *Column (a) - Original images with hair features [16]. Column (b) - Images resulting after Black Hat Transform morphological operation, with the following values for kernel1 = kernel2 = 28 x 28 and kernel3 = 9 x 9. Column (c) - The images resulting after the inpainting step where the hair was removed.*

Additional visual results are displayed in Figure 3 where the proposed hair removal procedure was applied to images with pronounced hair features belonging to HAM10000 database.

2.3. The segmentation method

In this paper, the hair removal pre-processing algorithm was used in conjunction with a binary segmentation procedure to facilitate the quantitative and qualitative evaluation of the hair removal procedure. Otsu's thresholding method [9] automatically calculates the optimal threshold value by maximizing the variance between the foreground and background pixels. This removes the need for manual adjustment of threshold values. Otsu's method is fast, easy to use, doesn't require user input, therefore it can serve as a benchmark for testing the effectiveness of various segmentation preprocessing steps.

By applying the automatic Otsu thresholding method [9] on the resulting inpainted

image, provides an effective way to test the hair removal algorithm as the Otsu method separates the image into distinct foreground and background classes by maximizing the separability between them. This method was selected as it removes the requirement of a user-defined threshold. To reduce the impact of the image noise, the inpainted image is subjected to a Gaussian filtering prior to the application of the Otsu thresholding algorithm.

3. Experiments and Results

The experimental procedure presented in this paper has a dual purpose. The first is to optimise the parameters involved during the Black Hat transformation and the following inpainting algorithm, while the second is to quantify the performance degradation inflicted by the hair artefacts present in the image. For the numerical evaluation, a database of 100 images with prominent hair features was extracted from the HAM10000 Dataset [16], a large collection of dermoscopic images of pigmented skin lesions collected from different populations and publicly available through the ISIC archive. This is a benchmark dataset that also offers the ground truth data marked by a medical professional. Some of the selected images used in this paper are displayed in Figure 1.

The experimental selection of the optimal kernel parameters involved in the Black Hat operation step of the hair removal algorithm was performed as follows: the values of *kernel1, kernel2* and *kernel3* were selected so that they maximize the following statistical metrics (while minimizing their mean standard deviation): accuracy (the results are displayed in Table 1), Dice measure (results displayed in Table 2), precision (results displayed in Table 3), recall (results displayed in Table 4) and F1 score (Table 5) of the segmented images when compared to the ground truth data. The tables below show that the optimal kernel parameters are: *kernel1 = kernel2 = 28x28* and *kernel3 = 9x9*.

During the inpaiting procedure, the threshold value that will be used to separate the pixel values into two classes (one for background and one for foreground) in this paper was set to 15 (th = 15). The numerical experiments used for the selection of this value are detailed in Table 6. The threshold value varied from 5 to 40 and the accuracy mean, Dice mean measure, precision mean, recall mean and F1 score mean were computed. The optimal threshold value was selected as the one that maximized the statistical measures while at the same time minimizing the standard deviation.

Using these optimal values, the algorithm discussed in this paper was applied to the selected database of dermoscopic images and the overall statistical results are displayed in Table 7.

Because the main purpose of this paper is to demonstrate the improved accuracy of the segmentation algorithm when applying the hair removal operation, the numerical statistical values when the hair removal algorithm was not applied prior to the segmentation step were also calculated and included in Table 7, for comparison purposes. The addition of the hair removal operation presented in this paper has increased the overall accuracy of the segmentation algorithm from 0.886 to 0.907, the Dice measure increased from 0.739 to 0.827, while the F1 score has increased from 0.847 to 0.937. Additional results are also shown in Table 7.

Accuracy Mean/ Accuracy Standard Deviation for varying kernel values Table 1

Kernel3 \ Kernel2	**7x7**	**14x14**	**21x21**	**28x28**	**35x35**
3x3	0.877/0.128	0.893/0.105	0.899/0.091	0.898/0.094	0.897/0.094
6x6	0.867/0.136	0.896/0.098	0.906/**0.080**	0.903/0.090	0.901/0.094
9x9	0.859/0.139	0.900/0.093	0.906/0.081	**0.907/**0.081	0.905/0.081

Dice Mean /Dice Standard Deviation for varying kernel values Table 2

Kernel3 \ Kernel2	**7x7**	**14x14**	**21x21**	**28x28**	**35x35**
3x3	0.726/0.280	0.780/0.211	0.783/0.207	0.785/0.207	0.784/0.208
6x6	0.677/0.326	0.790/0.196	0.824/**0.111**	0.818/0.138	0.810/0.160
9x9	0.635/0.356	0.792/0.197	0.819/0.137	**0.827/0.111**	0.823/0.116

Precision Lesion Mean/Precision Lesion Standard Deviation Table 3

Kernel3 \ Kernel2	**7x7**	**14x14**	**21x21**	**28x28**	**35x35**
3x3	0.670/0.253	0.720/0.185	0.719/0.186	0.723/0.184	0.724/0.184
6x6	0.628/0.297	0.729/0.171	0.760/0.081	0.757/0.109	0.750/0.132
9x9	0.590/0.325	0.726/0.171	0.754/0.109	0.763/0.080	**0.766/0.081**

Recall Lesion Mean/Recall Lesion Standard Deviation Table 4

Kernel3 \ Kernel2	**7x7**	**14x14**	**21x21**	**28x28**	**35x35**
3x3	0.826/0.335	0.886/0.264	0.892/0.257	0.890/0.258	0.887/0.260
6x6	0.767/0.385	0.897/0.248	0.935/0.169	0.935/0.171	0.914/0.214
9x9	0.720/0.417	0.904/0.246	0.929/0.190	**0.937/0.168**	0.928/0.180

F1_score Lesion Mean/ F1_score Lesion Standard Deviation Table 5

Kernel3 \ Kernel2	**7x7**	**14x14**	**21x21**	**28x28**	**35x35**
3x3	0.826/0.335	0.886/0.264	0.892/0.257	0.890/0.258	0.887/0.260
6x6	0.767/0.385	0.897/0.248	0.935/0.169	0.935/0.171	0.914/0.214
9x9	0.720/0.417	0.904/0.246	0.929/0.190	**0.937/0.168**	0.928/0.180

Table 6

The experimental selection of the threshold value (th) employed during the inpainting procedure. Best results were obtained for th = 15

Results / Threshold	*Accuracy Mean/st_dev*	*Dice Mean/st_dev*	*Precision Lesion Mean/st_dev*	*Recall Lesion Mean/st_dev*	*F1_score Lesion Mean/st-dev*
th = 5	0.904/0.082	0.816/0.134	0.752/0.112	0.925/0.190	0.925/0.190
th = 10	0.905/0.082	0.823/0.114	0.764/0.081	0.931/0.176	0.931/0.176
th = 15	**0.907/0.081**	**0.827/0.111**	**0.763/0.080**	**0.937/0.168**	**0.937/0.168**
th = 20	0.906/0.083	0.825/0.113	0.760/0.086	0.937/0.167	0.937/0.167
th = 25	0.907/0.080	0.827/0.110	0.763/0.078	0.936/0.167	0.936/0.167
th = 30	0.906/0.080	0.818/0.137	0.755/0.110	0.927/0.190	0.927/0.190
th = 40	0.899/0.092	0.791/0.196	0.730/0.170	0.898/0.248	0.898/0.248

Overall statistics: mean and standard deviation (st_dev) Table 7

Hair Removal Algorithm Applied	Accuracy Mean/ Accuracy st_dev	Dice Mean /Dice st_dev	Precision Mean/ Precision st_dev	Recall Mean/ Recall st_dev	F1 -score Mean/ F1-score st_dev
YES	**0.907/0.081**	**0.827/0.111**	**0.763/0.080**	**0.937/0.168**	**0.937/0.168**
NO	0.886/0.110	0.739/0.268	0.682/0.246	0.847/0.303	0.847/0.303

Table 8 presents the computational efficiency of the algorithm. The results demonstrate that the algorithm operates with consistent performance across different images. Specifically, the minimum processing time was recorded at 0.0124 seconds, while the maximum processing time reached 0.0503 seconds, indicating that the algorithm's execution time remains relatively stable under various conditions. The mean processing time across all images was 0.0277 seconds, suggesting that, on average, the algorithm completes its task in approximately 27.7 milliseconds. Furthermore, the standard deviation of the processing times was found to be 0.0086 seconds, reflecting a moderate level of variance in execution time. Overall, the results highlight the algorithm's ability to process data efficiently, making it well-suited for applications requiring time efficient execution.

Table 8

Computational efficiency and the overall processing time of the hair removal algorithm. The implementation was conducted using Python

Processing time minimum	Processing time maximum	Processing time mean	Processing time standard deviation
0.0123 s	0.0502 s	0.0277 s	0.0086 s

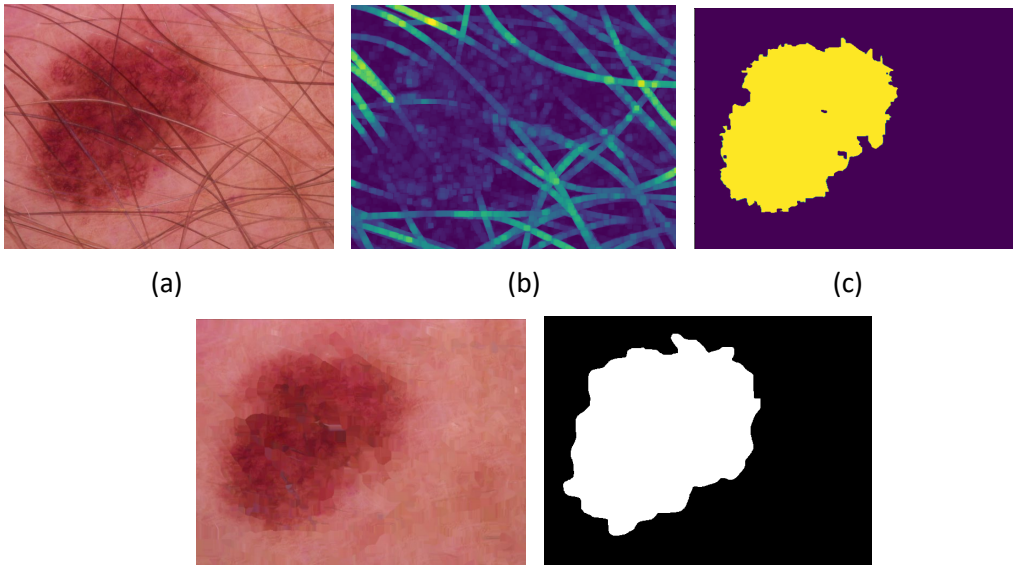

Fig. 4. *(a) Original image [16]. (b) Image resulting after Black Hat Transform morphological operation, with the following values for kernel1=kernal2=28x28 and kernel3 = 9x9. (c) The image resulting after the inpainting step where the hair was removed. (d) The segmentation result. (e) original Ground Truth image. Overall statistics: Accuracy = 0.94, Dice = 0.90, Precision_lesion = 0.82, Recall_lesion = 0.99, F1_score_lesion = 0.99*

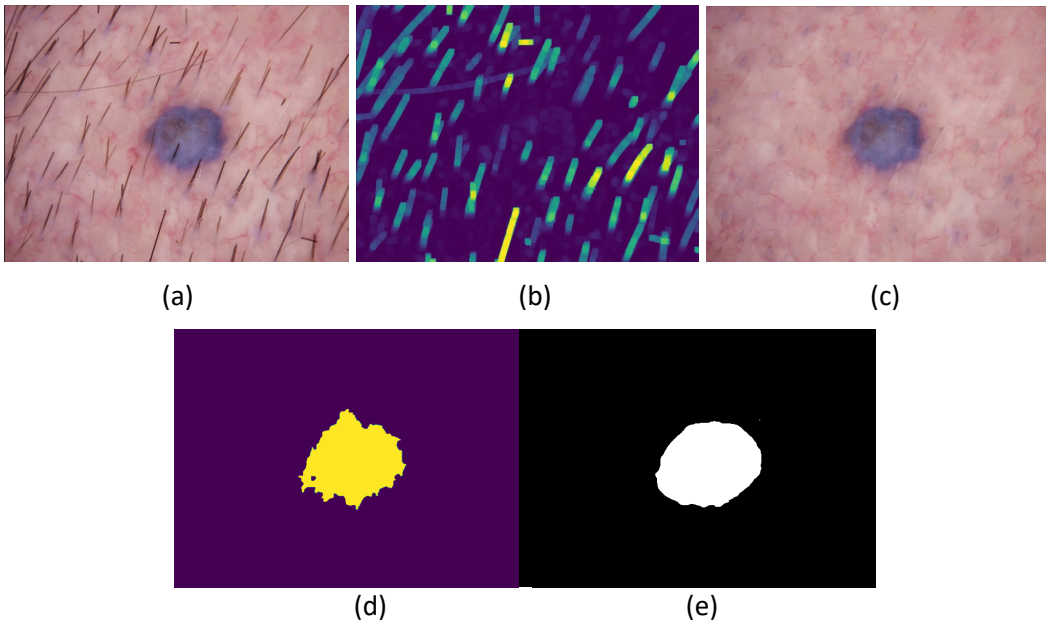

Fig. 5. *(a) Original image [16]. (b) Image resulting after Black Hat Transform morphological operation. (c) The image resulting after the inpainting step where the hair was removed. (d) The segmentation result. (e) original Ground Truth image. Overall statistics: Accuracy = 0.98, Dice = 0.91, Precision_lesion = 0.87, Recall_lesion = 0.97, F1_score_lesion = 0.97*

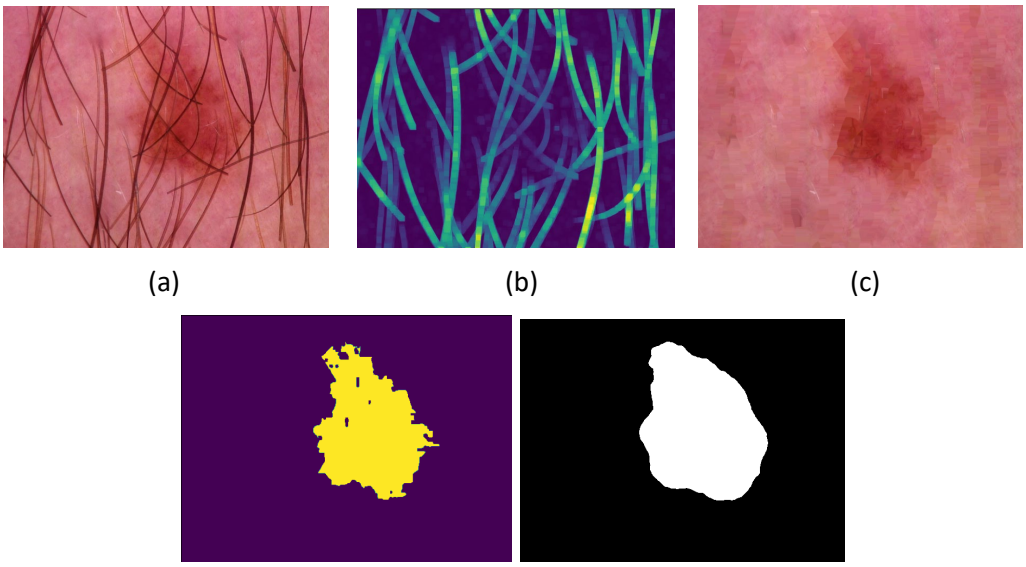

Fig. 6. *(a) Original image [16]. (b) Image resulting after Black Hat Transform morphological operation, with the following values for kernel1 = kernel2 = 28x28 and kernel3 = 9x9. (c) The image resulting after the inpainting step where the hair was removed (d) The segmentation result and (e) original Ground Truth image. Overall statistics:* Accuracy = 0.95, Dice = 0.85, Precision_lesion = 0.74, Recall_lesion= 0.99, *F1_score_lesion* = 0.99.

The step by step aplication of the algorithm discussed in this paper is visually displayed in Figures 4 - 6 numerically evaluated using the following statistical measures: accuracy, Dice measure, precision, recall and F1 score for the lesion region.

4. Conclusions

This paper emphasizes the importance of the hair removal pre-processing step in the skin cancer image segmentation process and it proposes an efficient automatic hair removal strategy with optimal parameters selection and a comprehensive quantitative evaluation of the obtained results. The experimental results demonstrate improved accuracy in the performance of automated skin cancer detection system, highlighting the potential of this approach for clinical applications in dermatology.

References

1. Barin, S., Güraksin, G. E.: *An improved hair removal algorithm for dermoscopy images.* In: Multimedia Tools and Applications (2024), Vol. 83(3), p. 8931-8953.
2. El-Shafai, W., El-Fattah, I. A. & Taha, T. E.: *Deep learning-based hair removal for improved diagnostics of skin diseases*. In: Multimedia Tools Applications, Vol. 83, p. 27331–27355.

3. Jütte, L., Patel, H., Roth, B.: *Advancing dermoscopy through a synthetic hair benchmark dataset and deep learning-based hair removal*. In: Journal of Biomedical Optics (2025), Vol. 29(11), 116003.
4. Kasmi, R. et al: *SharpRazor: Automatic removal of hair and ruler marks from dermoscopy images*. In: Skin Research and Technology (2023), Vol. 29(4), e13203.
5. Kaur, R., Gholam Hosseini, H., Lindén, M.: *Advanced Deep Learning Models for Melanoma Diagnosis in Computer-Aided Skin Cancer Detection*. In: Sensors (2025), Vol. 25, 594.
6. Kiani, K., Sharafat A.R.: *E-shaver: An improved DullRazor® for digitally removing dark and light-colored hairs in dermoscopic images*. In: Computers in Biology and Medicine (2021), Vol. 41(3), p. 139-145.
7. Lama, N., Kasmi, R. et al: *ChimeraNet: U-Net for Hair Detection in Dermoscopic Skin Lesion Images*. In: Journal Digital Imaging (2023), Vol. 36(2), p. 526-535.
8. Lee, T., Ng, V. et al: *DullRazor: a software approach to hair removal from images*. In: Computers in Biology and Medicine (1997), Vol. 27(6), p. 533-543.
9. Otsu, N.: *A threshold selection method from gray-level histograms.* In: IEEE Transactions on Systems, Man, and Cybernetics (1979), Vol. 9(1), p. 62–66.
10. Priyeshkumar, A. T., Shyamala, G., et al.: *Transforming Skin Cancer Diagnosis: A Deep Learning Approach with the Ham10000 Dataset*. In: Cancer Investigation (2025), Vol. 42(10), p. 801–814.
11. Quishpe-Usca, A., Cuenca-Dominguez, S., et al: *The effect of hair removal and filtering on melanoma detection: a comparative deep learning study with AlexNet CNN*. In: PEERJ COMPUTER SCIENCE (2024), Vol. 10, e1953.
12. Ramella, G.: *Hair Removal Combining Saliency, Shape and Color*. In: Applied Sciences (2021), Vol. 11(1), 447.
13. Suryanarayana, V., Prabhu Shankar, B., et al: *Effects of objects and image quality on melanoma classification using Spatio Temporal Joint Graph Convolutional Network*. In: *Biomedical Signal Processing and Control* (2025), Vol. 101, 107193.
14. Talavera-Martínez, L., Bibiloni P., González-Hidalgo, M.: *Hair Segmentation and Removal in Dermoscopic Images Using Deep Learning.* In: IEEE Access (2021), Vol. 9, p. 2694-2704.
15. Telea, A.: *An Image Inpainting Technique Based on the Fast Marching Method*. In: Journal of Graphics Tools, Vol. 9(1), p. 23–34.
16. Tschandl, P., Rosendahl, C. & Kittler, H. *The HAM10000 dataset, a large collection of multi-source dermatoscopic images of common pigmented skin lesions*. In: *Sci Data* **5**, 180161 (2018). https://doi.org/10.1038/sdata.2018.161
17. https://www.wcrf.org/preventing-cancer/cancer-statistics/skin-cancer-statistics/#latest-skin-cancer-data Accessed 24.02.2025.